In Situ Encapsulation of Tetradecane Droplets in Oil-in-Water Emulsions Using Amino Resins

Martin Sgraja,[1] Jan Blömer,[1] Jürgen Bertling,[1] Peter J. Jansens[2]

[1]*Department of Advanced Materials, Fraunhofer Institute for Enviromental, Safety, and Energy Technology UMSICHT, Osterfelder Str. 3, 46047 Oberhausen, Germany*
[2]*Department of Process and Energy Laboratory, Delft University of Technology, Leeghwaterstraat 44, 2628 Delft, The Netherlands*

Received 19 December 2006; accepted 6 March 2008
DOI 10.1002/app.28329
Published online 18 August 2008 in Wiley InterScience (www.interscience.wiley.com).

ABSTRACT: Microcapsules of tetradecane enclosed by a polymeric wall of amino resin were synthesized by the *in situ* polymerization using melamine-formaldehyde precondensates. It was found that resin concentrations of 60–240 g L^{-1} for a phase volume fraction of 0.14 and 0.29 and concentrations of 50–240 g L^{-1} for a phase volume fraction of 0.43 lead to stable microcapsules. Furthermore, the dependence of the shell thickness from the resin concentration for a phase volume fraction of 0.29 was investigated whereas the shell thickness was calculated from the density and the mean diameter of the capsules. It was found that below a concentration of 100 g L^{-1} the density and thus the shell thickness increases linear with the resin concentration whereas at higher concentrations it almost remains constant and only the amount of the resin precipitated in solution increases. Additionally, it was shown that the mean droplet size (which is almost equal to the capsule size) in dependence of the stirring speed can be derived from the theory of droplet disruption. Thereby the coherence beginning with the stirring speed and the mean diameter to the total surface and the shell thickness is described. © 2008 Wiley Periodicals, Inc. J Appl Polym Sci 110: 2366–2373, 2008

Key words: microencapsulation; resins; emulsions; phase diagrams; density

INTRODUCTION

Since the development of microcapsules and their application for carbonless copying papers the field of microencapsulation has remarkably increased. The wide spread of microcapsules is based on the fact that microcapsules fulfill a lot of different requirements due to the specific combination of the properties of a core and a wall material.[1–4] Microcapsules are used for the protection of the core material from the environment (e.g., the protection of a flavor against oxidation which is used in the food industry[1]), the protection of the environment from the core material (e.g., encapsulated contrast agents for diagnostic purposes used in medicine[2]) and controlled release applications.[3] Another field of application which has attracted growing interest in the last years is the synthesis of phase change materials (PCMs). PCMs contain encapsulated oils or waxes (especial higher hydrocarbons like tetradecane) with the capability to store energy in the form of latent heat in the solid-liquid phase transition.[5,6] They can be applied for example in heat absorbing paints as well as in heating and cooling pads in medicine and textile products.

One class of wall materials which is frequently used for microencapsulation are amino resins (especially resins of melamine and formaldehyde) which are low-priced and easy to handle. For microcapsules based on amino resins an *in situ* encapsulation process, which is well described in literature,[7–14] is used. In this process an emulsion or suspension of the core material, depending on whether a liquid or a solid material has to be encapsulated, is formed. Subsequently, the prepolymers are added to the continuous phase and the pH is lowered to 3–4. Because of the surface activity of the resin an enriched phase at the interface is formed. Afterwards, in the polycondensation step at elevated temperature the prepolymers are undergoing polymerization, favored in the enriched phase. Thereby, the hydrophobicity of the polymer increases until it precipitates in the form of particles at the surface of the dispersed phase forming a three dimensional crosslinked polymer wall.

Two important points, little treated in literature, are the wall thickness and the capsule size which define the mechanical stability, the release rate or barrier properties and the maximum load of active components in the application. The wall thickness is controlled by the amount of wall material with

Correspondence to: M. Sgraja (martin.sgraja@umsicht.fraunhofer.de).

© 2008 Wiley Periodicals, Inc.

respect to the total surface of the core phase. The total surface area of a solid core material is given by the particle size distribution and the volume of particles. In case of a liquid core phase the total surface area of the droplets is defined by the droplet distribution which depends on the energy dissipation of the stirrer and the interfacial tension between the core and the continuous phase.

Aim of this article is, firstly, to define a process range in which the *in situ* encapsulation using oil-in-water (o/w) emulsions with tetradecane as the core and amino resins as the wall material is possible and mechanically stable microcapsules are yielded. The process range is defined by the phase volume fraction of the volume of the dispersed phase to the total volume $\phi_d = V_d\ (V_d + V_c)^{-1}$ and the concentration of the wall material with respect to the volume of the dispersed phase $c_w = m_w\ V_d^{-1}$. Phase volume fractions of 0.14, 0.29, and 0.43 and resin concentrations between 30 g L^{-1} and 300 g L^{-1} were used. Secondly, the wall thickness in dependence of the wall concentration is determined for a fixed phase volume fraction of $\phi_d = 0.29$ and a method to calculate the shell thickness in dependence of the density and the Sauter-diameter of the capsule is presented. Finally, the experimental droplet sizes (which were assumed to be equal to the measured capsule sizes) were compared to values gained from the theory of droplet disruption. It is shown that the theory, taking into account the stirrer geometry and the interfacial tension, can be used to estimate the mean droplet and capsule sizes, respectively.

MATERIALS AND METHODS

Materials

Poly(ethylene glycol) with an average molecular weight of 400 g L^{-1} was purchased from Fluka Chemical Co. (Baus, Switzerland). Citric acid, anhydrous for synthesis, was purchased from Merck Schuchardt Co. (Hohenbrunn, Germany). Methanol etherified melamine-formaldehyde precondensates with a solids content of 87% were provided by Cytec Industries BV (Botlek-Rotterdamm, The Netherlands). Tetradecane (Linpar 14) was purchased from Condea (Duisburg, Germany). All chemical agents were of analytical grade and were used without further purification. For the separation of the microcapsules a cellulose filter with an average pore size of 2.5 μm, purchased from Whatman International Ltd (Maidstone, England), was used.

Synthesis of microcapsules

For the synthesis of the capsules (Fig. 1) initially three solutions *viz*. the continuous aqueous phase, the dispersed tetradecane phase, and the solution containing the amino resin were prepared. For the continuous phase 1.2 g poly(ethylene glycol) acting as a protective colloid (stabilization by depletion) was dissolved in water. The amount of water used together with the volume of tetradecane made up a total volume of 120 mL. Afterwards the solution containing the protective colloid and the tetradecane were both heated to 60°C. After heating, the two liquids were mixed and emulsified at the same temperature for 10 min using a Polytron 1300D (Kinematica AG, Switzerland) at 12,000 rpm. In parallel the appropriate amount of wall material was diluted with distilled water to a total volume of 20 mL resulting in a total encapsulation volume of 140 mL. The adjustment of the wall material solution to a pH of about 3 was done shortly before the end of the first emulsification and thus the addition of the solution to prevent preliminary polycondensation and thus different starting conditions. After the addition of the wall material the emulsion was further emulsified for 10 min before the capsule walls were hardened while stirring the solution with a magnetic stirrer (300 rpm) at 60°C for 2 h. The capsules were subsequently filtrated, washed twice with about 200 mL distilled water, and dried under ambient conditions.

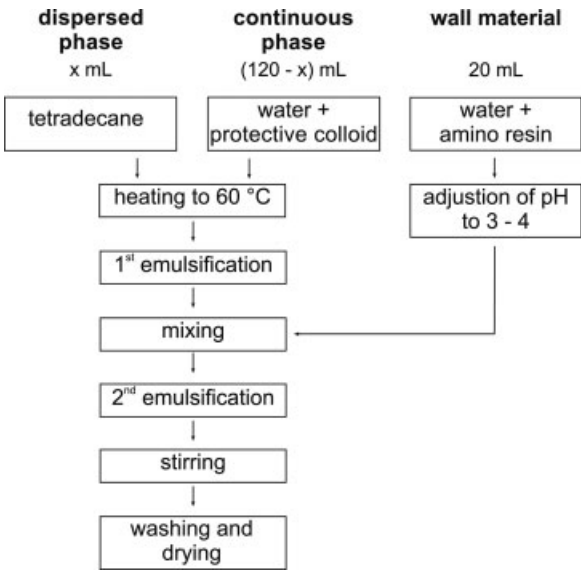

Figure 1 Flow chart of the synthesis of microcapsules.

Characterization

The particle size distributions of the capsules were determined by static light scattering (Mastersizer 2000, Malvern Instruments) using the Fraunhofer model for the analysis of the data. For investigation of the capsule morphology scanning electron microscopy (SEM, ESEM Quanta 400, Fei Company) was used. Prior to SEM investigations the samples had

been coated with a thin conducting layer of a gold/palladium (80/20%) (Sputter Coater K550, Fa. Emitech). The density determination of the capsules was performed using a He-gaspycnometer (Pycnomatic, Porotec). The surface and interfacial tension was determined using a tensiometer (DCAT 21, Dataphysics) whereas the interfacial tension was measured at 60°C to correspond to the encapsulation conditions. Here, the difficulty occurs that at higher concentrations, during the heating of the resin solution, polycondensation already occurs. Thus, the resin solutions were quickly heated to the desired temperature (60 ± 2°C) and the measurement was performed as fast as possible to reduce the effect of formed polymeric structures.

Determination of the wall thickness

For the determination of the wall thickness the microcapsules had to be separated from the amino resin precipitated in solution and not contained in the capsule wall. For this purpose, the capsule suspension was diluted with demineralised water to about 250 mL and centrifuged at 3000 rpm (Megafuge 1.0, Heraeus Sepatech Co.). The sediment was discarded and the creamed capsules together with the supernatant liquid were centrifuged again. The process was repeated up to three times until no more sedimented product could be found. Afterwards the suspension was filtrated through a 2.5 μm filter and the capsules were dried under ambient conditions. Determination of the density of the capsules was done by using a gas pycnometer with helium as the measurement gas. The shell thickness was calculated from the density of the capsules, lying between the density of pure tetradecane ($\rho_{d,20°C}$ = 0.7628 g/cm^3)[15] and that of the pure precipitated resin (1.56 g/cm^3). The density of the pure resin was determined on the basis of a performed microencapsulation without using a core material. For the calculation of the shell thickness from the density of the microcapsules it was assumed that the shell thickness is independent of the capsule size. This is justifiable since the wall material is dissolved in the continuous phase and the adsorption process is not dependent on the droplet size. For a capsule with a radius r_{d+w} containing a liquid droplet with the radius r_d, the shell thickness s can be defined as $s = r_{d+w} - r_d$. The radius of the capsule can be calculated as half of the surface weighted mean diameter $d_{3,2}$ gained from laser diffraction analysis. In consequence, the following equations describing the density of a capsule ρ_{d+w} by means of the mass of the core m_d and the wall m_w can be derived.

$$\rho_{d+w} = \frac{m_d + m_w}{V_{d+w}} \tag{1}$$

$$m_d = \frac{4}{3}\pi\gamma_d^3\rho_d; \quad m_w = \frac{4}{3}\pi\left(\gamma_{d+w}^3 - \gamma_d^3\right)\rho_w \tag{2a, b}$$

By combining the radius of the capsules r_{d+w} obtained from eqs. (2a), (2b) with the shell thickness s, the shell thickness in dependence of the density can be derived.

$$S = \frac{d_{3,2}}{2} \cdot \left(1 - \sqrt[3]{\frac{\rho_w - \rho_{d+w}}{\rho_w - \rho_d}}\right) \tag{3}$$

Droplet formation in the microencapsulation process

An important factor affecting the properties of the microcapsules is the preparation of the emulsion. By controlling the droplet size distribution the specific surface of the core phase and thus, by a given amount of wall material, the wall thickness can be defined.

Mersmann and Groβmann[16] as well as Karbstein[17] have shown that the process of droplet disruption can be described by the turbulent Weber number and the Ohnesorge number. In case of similar viscosities of the dispersed and the continuous phase ($\eta_{C_{14}H_{30},25°C}$ = 2.1 mPa s; $\eta_{H_2O,25°C}$ = 0.9 mPa s) internal fluiddynamic effects of the droplet can be neglected and the process of droplet disruption can be described by the Weber number only. Combining the stirrer Weber number We_{stir} (4) with the turbulent fluctuation velocity $u \sim (\varepsilon\, x_{max})^{1/3}$ taken from the theory of Kolmogorov[18] and expressing the local energy dissipation ε by the stirrer diameter L and the stirring rate n ($\varepsilon \sim n^3\, L^2$) Eq. (5) is obtained.

$$We_{stir} = const. = u^2\, x_{max}\, \rho_f/\gamma \tag{4}$$

$$x_{max} \sim \left(\gamma^{-1}\, n^2\, L^{4/3}\, \rho_f\right)^{-0.6} \tag{5}$$

Here, x_{max} is the maximum droplet diameter, γ the interfacial tension between the two liquids and ρ_f the density of the continuous phase. It was found experimentally that the maximum droplet diameter can be exchanged by the Sauter diameter $d_{3,2}$ which in most cases can be assumed to be directly proportional to the maximum droplet size. By adding the term ($1 + C_2\phi_d$, $C_2 \approx 3$) describing the decay of the turbulence and a second proportionallity constant $C_1 \approx 0.05$ Eq. (6) is formed.[19]

$$d_{3,2} = C_1\left(\gamma^{-1}\, n^2\, L^{4/3}\, \rho_f\right)^{-0.6}(1 + C_2\phi_d) \tag{6}$$

This equation thus gives the possibility to calculate the average droplet size from the interfacial tension between the two liquids as well as the stirring speed

and the diameter of the stirrer. In case of premixed phases the density is replaced by the average density of the system $\rho_f = \rho_c (1 - \phi_d) + (\rho_d \phi_d)$.[19] For the measurement of the experimental droplet sizes the droplets were encapsulated to stabilize them against coalescence. The microencapsulation process was performed at a phase volume fraction of 0.29 and a resin concentration of 80 g L^{-1}. For the emulsification a Polytron PT3100 (Kinematica AG, Switzerland), with the same stirrer diameter as the PT1300, was used. Here, the stirrer speed was varied between 8,000 and 18,000 rpm without changing the engine. However, in contrast to the previously described encapsulation scheme the mean capsule diameter was directly measured after the second emulsification step, since the encapsulation step was only used to stabilize the emulsion. As will be shown in the following, the maximum wall thickness under the given conditions is 100 nm. This means that the size difference between the droplet and the capsules (assuming a mean diameter of 10 μm and a broad size distribution) is within the measurement accuracy of the laser diffraction. Thus, the difference will be neglected considering the capsule size as the droplet size.

RESULTS AND DISCUSSION

Determination of the process range for encapsulation

The first step in the investigation of the microencapsulation process was the determination of a process range with respect to the volume fraction and the resin concentration in which microencapsulation is possible and mechanically stable microcapsules are obtained. For this purpose, the microencapsulation process was performed using different phase volume fractions (ϕ_d = 0.14, 0.29, 0.43) and resin concentrations (c_w = 30 g L^{-1} − 300 g L^{-1}). It was not possible to use higher volume fractions of tetradecane since the energy input of the stirrer was too low to emulsify the complete oil phase without using a surfactant. In Figure 2 the range in which microencapsulation is possible is displayed in form of a ternary [Fig. 2(A)] and a Cartesian diagram [Fig. 2(B)]. The open, half filled, and filled diamonds display the range where microencapsulation is possible, possible to a limited extend or not possible, respectively.

At a phase volume fraction of 0.14, it was found that even at concentrations of as little as 30 g L^{-1} microcapsules with a thin polymer wall are formed. However, after centrifugation and drying of the product the capsules are strongly agglomerated and show a waxy appearance. This means that a capsule wall is formed during the encapsulation, but in the centrifugation step the walls are partially broken and the tetradecane is released. Thus, the capsule wall is not stable enough to endure stress in practical applications. However, resin concentrations from 60 up to 240 g L^{-1} lead to mechanically stable microcapsules whereas in the upper range increased agglomeration of the capsules can be observed. Because of the formation of numerous colloidal resin particles a further increase of the concentration of the wall material above 240 g L^{-1} leads to a sharp rise of the viscosity of the system and accordingly to a gel-network consisting of the colloidal particles and capsules. This gel could not be suspended, filtrated, and dried to individual capsules anymore. At an increased phase volume fraction of 0.29 the same effects as at a phase volume fraction of 0.14 can be noticed. Below a resin concentration of 60 g L^{-1} the capsules do not withstand the mechanical stress during the centrifugation and drying step; in a

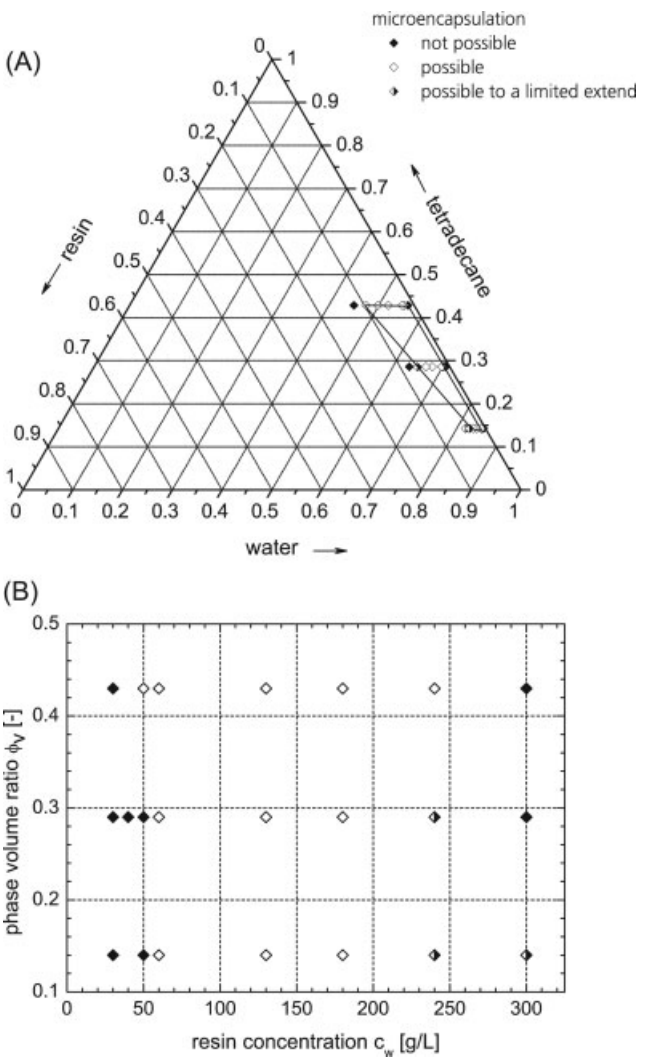

Figure 2 Ternary (A) and Cartesian (B) phase diagram showing the area of operation where microcapsules can be synthesized. The values given in the ternary diagram are weight percentages.

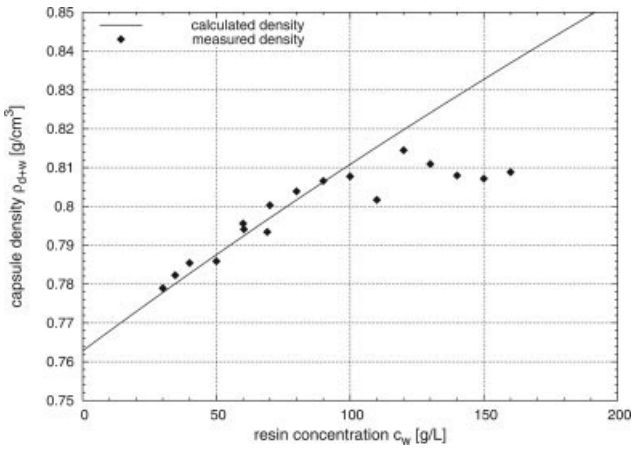

Figure 3 Comparison of the theoretical and measured capsule density.

concentration range between 60 and 240 g L^{-1} stable microcapsules are yielded and at concentrations higher than 240 g L^{-1} a gel consisting of resin particles precipitated in solution and microcapsules is formed. In further increasing the phase volume fraction to 0.43 almost the same effects can be seen. However, it was found that the concentration range for the synthesis of stable capsules was between 50 and 240 g L^{-1}. This slightly different range can be explained by the fact that the resin concentration is calculated with respect to the volume of the dispersed phase. When the volume of the dispersed phase is increased, the amount of wall material, at a constant concentration, is increased, too. The volume grows faster than the surface area and thus the minimum wall material is reached at lower concentrations. However, the exact determination of the borders of the process range is difficult since the evaluation of the stability criteria is not always unambiguous.

Dependence of the wall thickness from the resin concentration

In the second step of this work the dependence of shell thickness from the resin concentration was determined. A phase volume fraction of 0.29 and resin concentrations between 30 and 160 g L^{-1} were chosen. The microencapsulation was performed as described above and the density was measured using a He-pycnometer. It was found that the coefficient of variation of the density measurements was always better than $5 \cdot 10^{-4}$. In Figure 3 the measured density in comparison with the theoretical density $\rho_{theo} = (m_d + m_w)\,(V_d + V_w)^{-1}$, calculated on the basis of complete incorporation of the resin into the wall phase, is diagrammed.

It can be observed that at concentrations below 100 g L^{-1} the theoretical and experimental density match each other. Slightly higher measured densities than the theoretical density can be explained by loss of small amounts of tetradecane which shifts the measured density to higher values. However, at concentrations of more than 100 g L^{-1} the measured density remains almost constant. The curve progression indicates that at concentrations below 100 g L^{-1} all the resin is used for the wall formation, whereas at higher concentrations the excess material is precipitated in the solution without being part of a capsule wall. This means that in the encapsulation step when the enriched phase around the droplets is formed there is a maximum thickness of this layer due to the fact that the driving force for the enrichment is the decrease of the interfacial tension between the hydrophobic tetradecane and the hydrophilic water phase. Thus, under the given process conditions, there is no benefit in using resin concentrations exceeding 100 g L^{-1} for the microencapsulation process. Figure 4 displays SEM pictures of capsules synthesized with resin concentrations of 60 g L^{-1}, 100 g L^{-1}, and 150 g L^{-1} [Fig. 4 (A-C)]. It can be seen that the surface roughness of the capsules increases with increasing resin concentrations. With rising concentrations the number of resin particles precipitated in solution increases which lead to a higher surface roughness due to their incorporation into the wall or precipitation on the surface of the capsules.

Shell thickness in dependence of the resin concentration

As mentioned before the shell thickness is not only dependent on the amount of wall material but also on the specific surface of the emulsion. A typical surface weighted capsule size distribution with its characteristics, synthesized by the described process, is displayed in Figure 5.

It can be observed that the size distribution of the capsules consists of a small and a broad peak in the range of 1–5 μm and 5–45 μm, respectively. Because of the fact that there are two peaks, of which the second is very broad, the width $(d_{90} - d_{10})/d_{50} = 6.90$ and the uniformity (relative standard deviation) of the distribution (2.3) are very high. The small capsules, represented by the first peak, show approximately the same amount of surface as the larger capsules represented by the broad peak. The curve shows a volume and surface weighted mean diameter of $d_{4,3} = 19.7$ μm and $d_{3,2} = 9.4$ μm, respectively. The mass based specific surface area S_m was found to be 0.8 m^2 g^{-1} when a density of $\rho_{c+w} = 0.8$ g cm^{-3} was used for the calculation. It is worth noticing that the shown particle size distribution is independent of the resin concentration which can be understood when the surface tension in dependence of the resin concentration is taken into account (Fig. 6). Up to resin concentrations of about 30 g L^{-1}

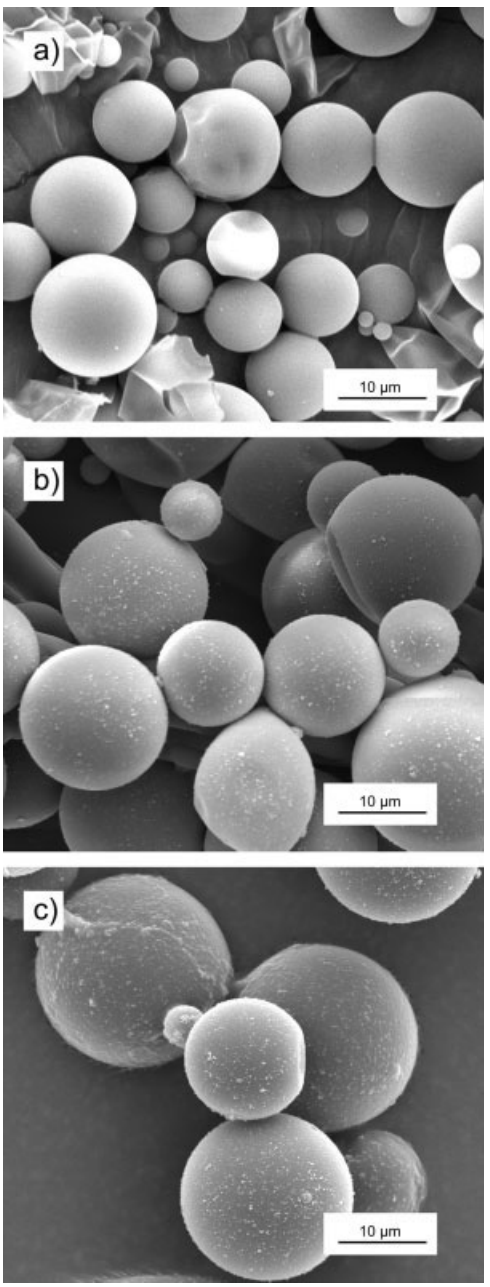

Figure 4 Scanning electron microscopy pictures of capsules synthesized using a resin concentration of 60 g L^{-1} (A), 100 g L^{-1} (B) and 150 g L^{-1} (C).

a strong decrease of the surface tension with growing resin concentration occurs. At higher concentrations, the concentration range used for encapsulation, the surface tension roughly remains constant. The same effect can be seen having a look at the interfacial tension between tetradecane and the resin solution (Table included in Fig. 6); it decreases from 20.0 mN m^{-1} at a concentration of 1 g L^{-1} to 12.2 mN m^{-1} at a concentration of 10 g L^{-1} but decreases only to a value of 11.2 mN m^{-1} by further increasing the concentration to 50 g L^{-1}. Thus, at resin concentrations of more than 30 g L^{-1} the surface and interfacial tension are

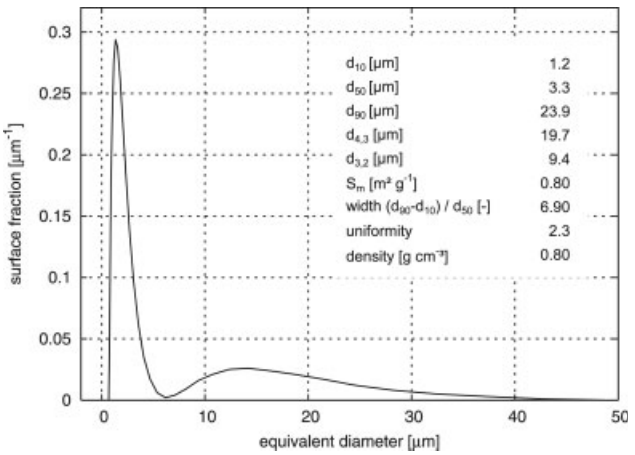

Figure 5 Typical particle size distribution of microcapsules and its characteristics.

almost constant leading to a constant droplet size distribution.

As described above the capsule size distribution and thus the surface weighted mean diameter is independent of the resin concentration. However, it was found that in repeated experiments under the same conditions the mean diameter varies due to slight changes within the experimental setup, e.g., position of the Polytron, and thus slightly changed velocity profiles. Since the wall thickness is derived from both the density and the measured Sauter diameter, which undergoes relatively large changes, the variance in the shell thickness is large, too. For this reason the shell thickness was plotted against the rate of the resin concentration to the total surface A of the droplet collective (Fig. 7). In addition to the points gained from experimental data theoretical curves for the theoretical density and the minimum (8.3 µm), the maximum (11.8 µm), and the average (9.5 µm) sauter diameter of all experiments are shown. In the present concentration range there is

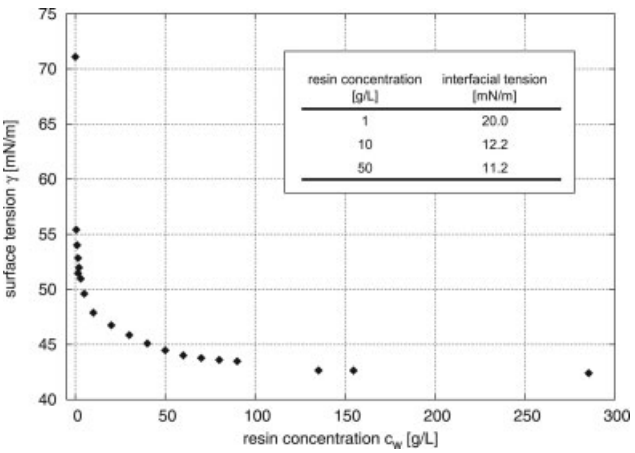

Figure 6 Surface and interfacial tension in dependence of the resin concentration.

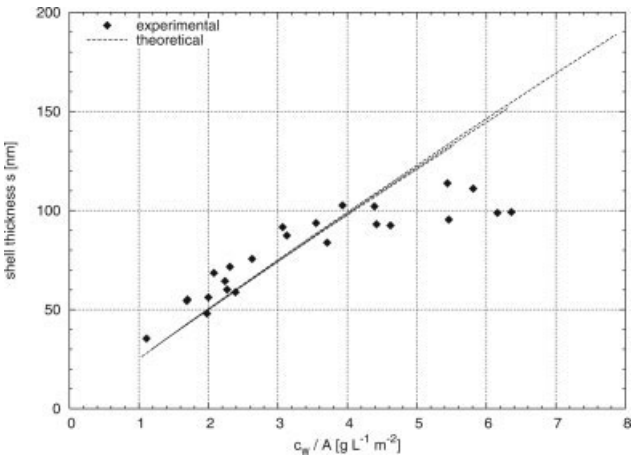

Figure 7 Shell thickness of microcapsules plotted against the rate of the resin concentration to the total surface area.

only a small deviance between the theoretical curves, which practically can be neglected.

Experimental points above the theoretical curve can be explained by the loss of small amounts of tetradecane, which leads to slightly higher density and thus to a larger shell thickness. Nevertheless, the same trend already indicated in Figure 3 can be observed here, too. At values of c_w/A less than 4 there is a linear increase of the shell thickness. It increases linearly from 30–100 nm with increasing wall concentration per total surface. At higher concentrations the shell thickness roughly remains constant, diverging from the theoretical curve. Thus, for the present size distribution, there is a maximum shell thickness of the capsule wall of about 100 nm.

Comparison of the theoretical and experimental droplet sizes

For the calculation of the theoretical mean droplet diameters first of all the interfacial tension between the resin solution and tetradecane was measured. The interfacial tension at 60°C was found to be 11.2 $\pm$ 0.4 mN m^{-1} (c_{resin} = 50 g L^{-1}) which is close to an interfacial tension of 8.6 mN m^{-1} for a triethanolamine modified melamine/formaldehyde resin (0.05 mol triethanolamine per mol melamine, measured at 20°C against xylene) published by Dietrich et al.[10] The interfacial tension together with the stirrer diameter ($L = 9 \times 10^{-3}$ m), the density of the liquid ρ_f = 931 kg/m^3 and the phase volume fraction of 0.43 was used to calculate the Sauter diameter in dependence of the stirrer speed (Fig. 8). In comparing the experimental points with the theoretical data it can be noted that the experimental points show the same characteristics as the theoretical curve (Fig. 8, solid line) whereas the points are shifted to larger diameters. However, it can be found that all the experimental points are in accordance with Eq. (6) when the exponent $y = -0.6$ is reduced by 4% to $y = -0.576$ (Fig. 8, dashed line). The deviation from the theoretical curve can be explained by the fact that that the assumption of isotropic turbulence, included in the theory of Kolmogorow, is not completely fulfilled in our system. Isotropic turbulence expresses that all flow directions are equal and that the degree of turbulence in each liquid cell is equal. In the experiments the energy input near the stirrer is much higher than in the vicinity of the vessel wall and additionally a flow profile is formed so that some flow directions are favored. Nevertheless, the equation gives the possibility to calculate the mean droplet size from the interfacial tension, the stirring rate, the stirrer diameter, the density and the phase volume fraction when the exponent of the equation is adapted to the experimental data.

CONCLUSIONS

Microcapsules with tetradecane as a core substance have been prepared using melamine-formaldehyde precondensates. It was found that for a phase volume fraction of 0.14 and 0.29 and a concentration range from 60 to 240 g L^{-1} and for a phase volume fraction of 0.43 and a concentration range of 50–240 g L^{-1} stable microcapsules could be synthesized. Subsequently, the density and the wall thickness in dependence of the resin concentration for a phase volume fraction of 0.29 were determined. It was found that for a resin concentration ranging from 30 to 100 g L^{-1} the density and the shell thickness increase linearly with the resin concentration ranging from 30 to 100 nm. Concentrations exceeding 100 g L^{-1} lead to an increased precipitation of the resin in so-

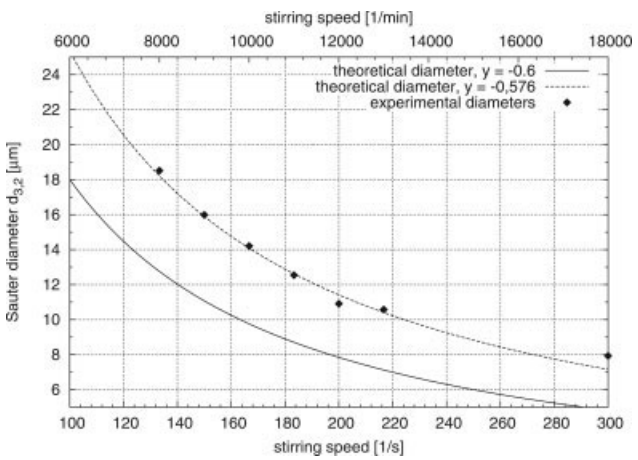

Figure 8 Experimental mean diameter in dependence of the stirring speed (filled diamonds) and the theoretical dependence of the mean diameter for an exponent of $y = -0.6$ (solid line) and a fitted exponent of $y = -0.576$ (dashed line).

lution and a wall thickness which remains almost constant. Finally, it was shown that the mean surface averaged capsule diameter (which is assumed to equal the droplet diameter) can be calculated from the interfacial tension, the stirring rate, the stirrer diameter, the fluid density and the phase volume fraction using an equation based on the theory of Kolmogorow. Here, the exponent ($y = -0.576$) was fitted to the experimental data taking into account that the flow profile is not ideal isotropic turbulent.

The results of this work show that the wall thickness of a capsule can be adjusted by controlling the stirring speed and the amount of the wall material. By setting up the stirrer speed and the mean droplet size the total interface can be set which controls the shell thickness of the capsules together with the amount of the wall material.

NOMENCLATURE

Symbols

A	total surface area of the droplets or capsules, m^2
c_w	concentration of the wall material based on the dispersed phase, g L^{-1}
C_1, C_2	constants
d_{10}, d_{50}, d_{90}	particle diameter corresponding to 10, 50, and 90% of the cumulative undersize distribution, m
$d_{3,2}$	surface weighted mean diameter, Sauter diameter, m
$d_{4,3}$	volume weighted mean diameter
L	stirrer diameter, m
M	mass, g
N	stirring rate, s^{-1}
r	radius, m
Re	Reynolds number
s	shell thickness, m
S_m	mass based specific surface, m^2 g^{-1}
u	turbulent fluctuation velocity, m s^{-1}
v	velocity, m s^{-1}
V	volume, L
We_{stir}	stirrer Weber number
x	droplet diameter, m
x_{max}	maximum droplet diameter, m

Greek symbols

γ	interfacial tension, mN m^{-1}
ε	energy dissipation, m^2 s^{-3}
η	dynamic viscosity, Pa s
ρ	density, g cm^{-3}
ρ_f	average fluid density, g cm^{-3}
ϕ	volume fraction (volume of the considered phase to the total volume)

Indices, subscripts

c	continuous phase
d	dispersed phase
$d + w$	microcapsule
f	fluid phase (dispersed and continuous phase)
w	capsule wall

References

1. Madene, A.; Jacquot, M.; Scher, J.; Desobry, S. Int Food Sci Technol 2006, 41, 1.
2. Sinha, V. R.; Goyal, V.; Bhinge, J. R.; Mittal, B. R.; Trehan, A. Crit Rev Ther Drug Carrier Syst 2003, 20, 433.
3. Arshadi, R.; Boh, B., Eds. Microspheres, Microcapsules and Liposomes Series 6; Citus Books: London, 2003.
4. Sgraja, M.; Bertling, J.; Kümmel, R.; Jansens, P. J. J Mat Sci 2006, 41, 5490.
5. Boh, B.; Knez, E.; Staresinic, M. J Appl Polym Sci 2005, 22, 715.
6. Su, J.; Wang, L.; Ren, L.; Huang, Z. J Appl Polym Sci 2006, 103, 1295.
7. Nastke, R.; Dietrich, K.; Reinisch, G.; Rafler, G. J Macromol Sci Chem 1986, A23, 579.
8. Dietrich, K.; Bonatz, E.; Geistlinger, H.; Herma, H.; Nastke, R.; Purz, H. J.; Schlawne, M.; Teige, W. Acta Polym 1989, 40, 325.
9. Dietrich, K.; Herma, H.; Nastke, R.; Bonatz, E.; Teige, W. Acta Polym 1989, 40, 243.
10. Dietrich, K.; Bonatz, E.; Nastke, R.; Herma, H.; Walter, M.; Teige, W. Acta Polym 1990, 41, 91.
11. Bonatz, E.; Dietrich, K.; Herma, H.; Nastke, R.; Walter, M.; Teige, W. Acta Polym 1989, 40, 683.
12. Kage, H.; Kawahara, H.; Hamada, N.; Kotake, T.; Oe, N.; Ogura, H. Adv Powder Technol 2002, 13, 377.
13. Lee, Y. H.; Kim, C. A.; Jang, W. H.; Choi, H. J.; Jhon, M. S. Polymer 2001, 42, 8277.
14. Lee, Y. H.; Lee, S. J.; Cheong, I. W.; Kim, J. H. J Microencapsul 2002, 19, 559.
15. Lide, D. R.; Frederikse, H. P. R., Eds.; Handbook of chemistry and physics, 78th ed.; CRC Press: New York, 1997.
16. Mersmann, A.; Groβmann, H. Chem Ing Tech 1980, 52, 621.
17. Karbstein, H.; Untersuchungen zum Herstellen und Stabilisieren von Öl-in-Wasser-Emulsionen, Ph.D. Dissertation, Universität Karlsruhe, 1994.
18. Kolmogorow, A. N. In Sammelband zur statistischen Theorie der Turbulenz; Goering, H., Ed.; Academie Verlag: Berlin, 1958.
19. Stiess, M. Mechanische Verfahrenstechnik 1, 2nd ed.; Springer: Berlin, 1995.